

# Radionuclide-Ligand-Solvent Systems in Fuel Reprocessing

Arya Das<sup>1,3</sup>, \*Sk. Musharaf Ali<sup>2,3</sup>

<sup>1</sup>Nuclear Recycle Board, Bhabha Atomic Research Centre, Mumbai-400085, India

<sup>2</sup>Chemical Engineering Group, Bhabha Atomic Research Center, Mumbai-400085, India

<sup>3</sup>Homi Bhabha National Institute, Mumbai-400094, India

### ABSTRACT

Spent fuel reprocessing is necessary to manage the nuclear fuel volume and also to produce the fresh fuel for fast reactor to maintain the closed fuel cycle. Various ligand-solvent systems are manipulated to achieve the best performance depending on the nature of the waste and type of the equipment. Therefore, one of the most crucial point is the selection of the ligand-solvent systems amongst myriads of ligands and solvents which is experimentally quite tedious and expensive. Molecular dynamics (MD) simulation and Quantum electronic structure calculation (QESC) have been emerged as virtual experimental methods for designing the effective ligand-solvent systems. Extensive calculations demonstrate that tri-iso-amyl phosphate (TiAP) is a viable alternative of tri-n-butyl phosphate (TBP) in the fuel reprocessing.

**Keywords:** Fuel reprocessing, Uranyl ion, TiAP, Dodecane, QESC, MD simulations.

### Introduction

Among the various sources of energy, nuclear energy shares ~15-20% of the total energy consumption worldwide. In view of the growing energy demand, fission-based nuclear power which has proven to be safe and reliable will play a vital role in meeting this need. One aspect of nuclear power that still provides significant technical challenges is the management of continuously increasing spent nuclear fuel in large volumes which necessitates the development of an effective and selective methodology for reuse by separation of actinides. Reprocessing of used nuclear fuel is of practical interest not only to reduce the high-active solid waste and its safe disposal but also to produce the fresh fuel for 2<sup>nd</sup> generation nuclear reactor.<sup>1</sup> The most commonly practiced extraction process is PUREX (Plutonium Uranium Recovery by Extraction) in which the Uranium and Plutonium are separated from aqueous solution obtained from the dissolution of irradiated fuel in nitric acid. The key extractant in PUREX process is tri-n-butyl phosphate (TBP) which is commonly used with dodecane as diluent. In spite of proven success of TBP as popular ligand; it has some inherent limitations that reduce the efficiency of the extraction process. Third phase formation in the extraction of Pu(IV), degradation due to radiological and chemical effects and the aqueous solubility are the serious issues with TBP. It is desirable to develop an alternate ligand

which has the advantages of TBP and mitigates the demerits of TBP.<sup>2</sup> Therefore, a detailed investigation on the structural and thermo-physical properties of pure ligands as well as in binary and biphasic mixture and the related dynamical properties for the metal extraction is of utmost necessary for better understanding of the extraction process.

To avoid various issues in performing experiments, molecular dynamics (MD) simulations and Quantum electronic structure calculations (QESC), which are very useful methods for investigating the microscopic structure and thermophysical properties are conducted. In past, several works have been carried out for the development of a force field which can predict the structural properties with suitable accuracy. For this purpose different atomic partial charges have been used to parameterize the force field in the last few decades. Recently, Cui *et al* have calculated the structural and thermophysical properties of TBP/dodecane mixture with two sets of force fields.<sup>3</sup> Mu *et al* stated that a single model cannot predict both the structural and thermo dynamical properties.<sup>4</sup> Cui *et al* reported that the structure is highly affected by the partial charge on TBP molecule.<sup>5</sup> Recently, Siu *et al* have refined the parameters of OPLS-AA (All-atom Optimized Potential for Liquid Simulations) force field for long hydrocarbons to reproduce the values of densities and heats of vaporization.<sup>6</sup> Vo *et al* worked for parameterization of force field based on the experimental density and the heat of vaporization.<sup>7</sup> Leay *et al* described the pathway of polar molecules from the aqueous phase to the organic phase through filament network.<sup>8</sup> Further, Mu *et al* have studied shear viscosity of TBP from non-equilibrium MD (NEMD) using periodic shear flow method.<sup>4</sup> Allen *et al* calculated the viscosity of alkanes from NEMD using parameterized OPLS model.<sup>9</sup> Though the parameterization of force field has been carried out based on density or dipole moment or heat of vaporization to calculate the structural and dynamical properties of ligand and ligand-solvent systems but it is case sensitive.

Further, it is equally important to study the behavior of TiAP/dodecane mixture in contact with aqueous phase in the presence of nitric acid. The calculation of interfacial properties are also required to understand the mass transfer through interface as it is difficult to explore the molecular details using experimental technique. Baaden *et al* have performed MD simulation focusing on the mixing and de-mixing of aqueous-organic solution and their interfacial distribution, but did not calculate the interfacial tension (IFT) and interface thickness (IFW).<sup>10</sup> Sahu *et al* have studied uranyl extraction using TBP and reported higher water extraction with

un-dissociated  $\text{HNO}_3$  compared to dissociated form of acid. The calculation of capillary thickness, total IFW and IFT was untouched. Furthermore, a considerable progress has been observed in the calculation of IFT using MD simulation in recent past.<sup>11</sup> Wen and co-workers revealed the increment of decane–water interfacial tension at low ionic concentration. They also did not focus on the calculation of IFW.<sup>12</sup> Biswas *et al* reported an enhancement of surface tension with the addition of metal salt.<sup>13</sup> Jorge *et al* estimated the total and intrinsic interface width for water–nitrobenzene system by fitting density profile where the proper prescription for calculation of total IFW is lacking and also not been addressed the presence of third component and acidity.<sup>14</sup> Senapati *et al* calculated the IFW and IFT of  $\text{CCl}_4$ /water system based on two different methods and computed the interface width by fitting the density curve but didn't study the effect of third component.<sup>15</sup> Hence, there are lots of ambiguity in the calculation of total and intrinsic interface thickness and no straightforward prescription is still available.

A theoretical and computational investigations on thermo-physical and dynamical behavior of aqueous actinides are essential because of the limitation in conducting the experiments due to radio-toxicity and also precise determination of their variable oxidation states and coordination numbers in aqueous solution. Earlier, several research groups have developed force field to model uranyl ion based on QM and MD simulations. Gulibaud and Wipff presented a theoretical study of uranyl ion in water.<sup>16</sup> Kerisit *et al* carried out simulations of  $\text{UO}_2^{2+}$  in water using GW and two other force fields to show that not a single model is able to predict the uranium–water oxygen distance or or hydration free energy.<sup>17</sup> Rai *et al* developed a force field using to establish the importance of using many body solvation effects for development of force field.<sup>18</sup> Therefore, concerns regarding the different charge models are really required to understand the hydrated uranyl ion. Further, literature reviews also depicted that the earlier studies on uranyl ion were carried out in water only. So, it is important to perform the studies in presence of nitric acid to reflect the practical experimental conditions.

The objective of the present article is to summarize the modified OPLS-AA force field using Mulliken, Löwdin, NPA (natural population analysis) and ChelpG (a grid based method using electrostatic potential) partial charge by studying the structural, thermo-dynamical and dynamical properties for pure TBP, TiAP and TEP which help in the screening of ligands for the extraction applications. Another objective is to test the calibrated force field in TiAP/dodecane binary mixture as well as in water–TiAP/dodecane biphasic mixture to see whether the force field is able to explain all the structural, thermo-dynamical and dynamical properties. An attempt has also been made for the calculation of total and intrinsic interface thickness for simple as well as complex biphasic mixture to understand the interfacial process. The versatility of force field is the main appeal of the current studies. The forth objective is to find out the effect of partial charges on actinides in water and then to calculate the various structural and dynamical properties of uranyl nitrate in nitric acid medium with wide range of uranyl nitrate as well as acid concentration.

### Computational Details

All the MD simulations were performed using GROMACS-4.5<sup>19</sup> package employing usual periodic boundary conditions and OPLS-AA force field. The initial molecular structures and partial charges on the each atom are computed at the B3LYP/TZVP<sup>20</sup> level of theory as implemented in TURBOMOLE<sup>21</sup> and GAMESS<sup>22</sup> packages. During

simulation, the long range electrostatic interactions are computed using particle mesh Ewald (PME)<sup>23</sup> method with an order of 6 and with a cutoff distance of 12Å. SPC/E<sup>24</sup> water model is used as it is more efficient compared to other models. The systems are equilibrated for 10ns in NPT ensemble with a time step of 2fs. Pressure of 1 atm is maintained using Berendsen like weak coupling methods and Velocity–rescaling thermostat is used to converge the temperature ( $T=300\text{K}$ ). Additional 10ns production run in NVT ensemble is performed.

### Results & Discussion

The ligands considered for study are generally optimized and then used for initial coordinate input in the MD simulation (Fig.1).

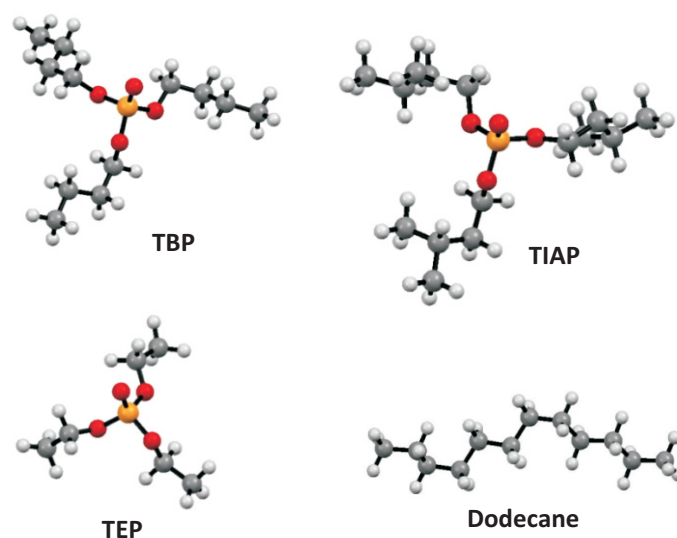


**Fig.1:** Optimized structures of ligand/solvent (red: O; orange: P; gray: C and white: H).

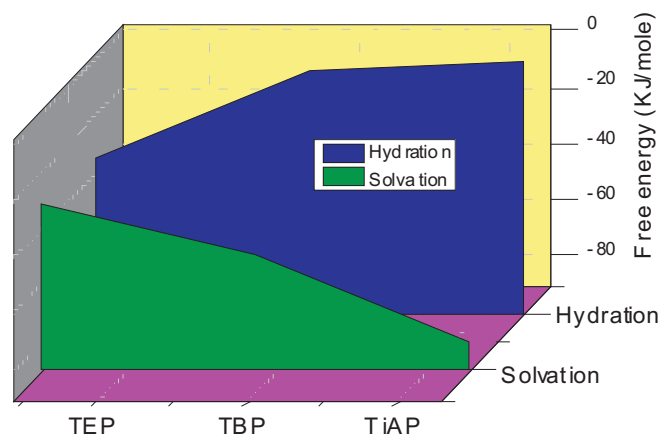


**Fig.2:** Calculated free energy of hydration and solvation for ligands in water and dodecane.

The calculated mass density, dipole moment and self-diffusivity of pure ligands using Mulliken population analysis are in good agreement with experimental data within 1% deviation indicating the best selection. Structural properties also support this fact. The acceptability of the Mulliken charge embedded force field further confirmed from the computation of  $\Delta G_{\text{Hydration}}$  and  $\Delta G_{\text{Solvation}}$  using Thermodynamic Integration (TI)<sup>25</sup> method. The screening of ligand has been carried out based on free energy and partitioning ability. The free energy studies exhibited the higher hydrophobic nature of TiAP compared to others and also higher degree of partitioning of TiAP in organic phase which are very much desirable for biphasic extraction<sup>26</sup> (see Fig. 2).

The larger the difference in hydration and solvation for TiAP, higher the free energy of transfer leading to higher partitioning of solute between two phases. The study also confirmed that TiAP has the higher partitioning ability. The increasing value of partition coefficient of alkyl phosphates with increasing alkyl groups is attributed to increasing hydrophobic alkyl group because the solubility of the tri-alkyl phosphates in water is decreased and increased in dodecane which in turn enhances the partitioning of the solute in dodecane. The heat of vaporization,  $\Delta H_{\text{vap}}$  of the liquid is in fair agreement with the experimental results. Finally the free energy of extraction,  $\Delta G_{\text{ext}}$  of  $\text{UO}_2^{2+}$  ion in water-dodecane system showed that the TiAP has the higher free energy of extraction than that of TBP which reflects the higher distribution constant of  $\text{UO}_2^{2+}$  ion with TiAP ( $D_{\text{U(VI)}}=29.8$ ) over TBP ( $D_{\text{U(VI)}}=24.5$ ) and hence TiAP might be used as an alternative of TBP.

Next, it is desirable to test the Mulliken embedded force field in binary mixture at various mole fraction of TiAP. The calculated densities are in good agreement with the experimental values signifies the accuracy of force field. Also, it correctly predicts the temperature effect on density of pure liquids and binary mixture with a deviation of 0.35-0.80%. The excess volume of mixing which signifies the interactions between the components of mixture was also calculated (Fig.3). The correct trend for excess volume of mixing confirms the accuracy of the force field.<sup>27</sup>

The structural properties reveal two possible orientations of neighbor TiAP molecules like

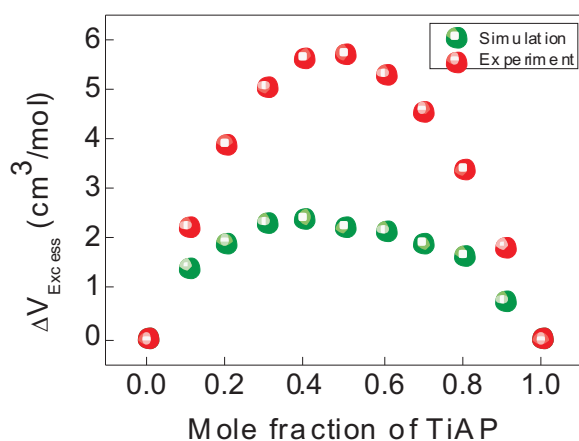
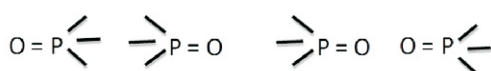


**Fig.3:** Excess volume of mixing of TiAP-dodecane.

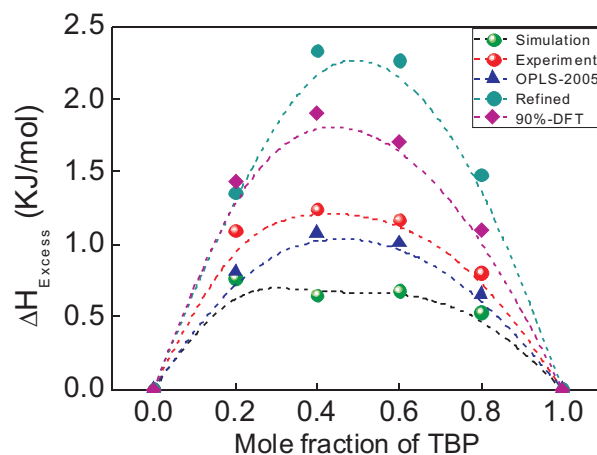


**Fig.4:** Excess enthalpy of TBP/dodecane mixture.

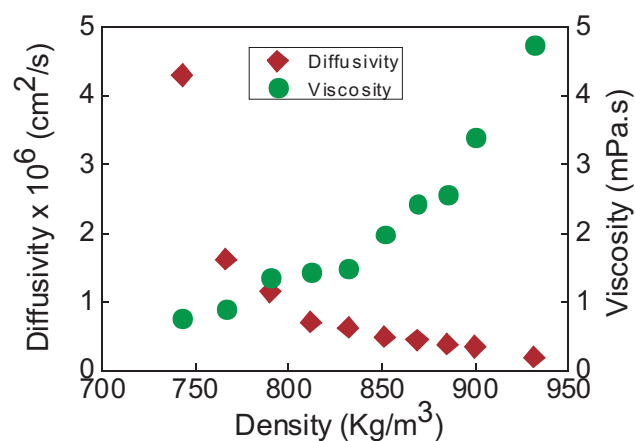


**Fig.5:** Diffusivity of TiAP and shear viscosity of TiAP-dodecane mixture as a function of density.

First one is from the hydrophobic side of the two different TiAP molecules and it is difficult to approach each other due to the large iso-amyl group and the second is from the phosphoryl group where the dipole-dipole interactions come into picture.<sup>27</sup> The calculation of excess enthalpy of mixing at different mole fraction of TBP predicts correctly the endothermic mixing as it was found experimentally (Fig.4). For TiAP also,  $\Delta H_{\text{Excess}}$  follows the trend and ensures the accuracy of developed force field.

The self-diffusivity (using Einstein's relation<sup>28</sup>) and shear viscosity (using periodic perturbation method from NEMD<sup>29</sup>) have been calculated. The dynamic properties of ligands play an important role in the mobility of the ligand which is a determining factor for the formation of metal-ligand complex. The effect of mole fraction of TiAP on self-diffusivity shows a decreasing trend with increasing mole fraction. The calculated viscosity of TBP is very close to the experimental value with a deviation of 0.25%, indicating a good accuracy of developed force field. For TiAP, it is  $4.74 \pm 0.03$  mPa.s (expt.:  $-4.27$  mPa.s). The shear viscosity of TiAP/n-dodecane binary mixture follows an increasing trend with mole fraction of TiAP.<sup>27</sup> The dynamic properties change with mole fraction. So, it is crucial to select the useful composition of TiAP/dodecane mixture to develop efficient extraction system. The low viscosity and high diffusivity are the major criteria for the selection of composition of any ligand-solvent system. The shear viscosity is shown to be an increasing function of mole fraction whereas diffusivity of TiAP is a decreasing function. So, it is important to select an optimum composition which is around 25–30% TiAP where the curves are intersecting each other as shown in Fig.5. This composition exhibits

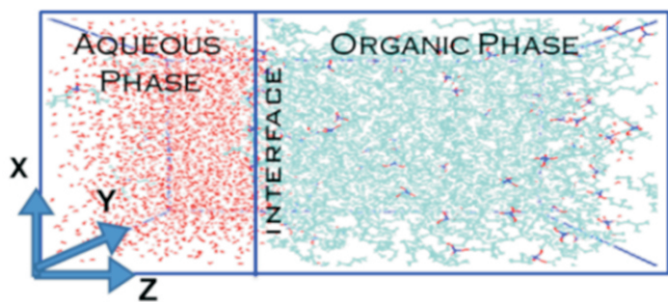


**Fig. 6:** A biphasic (organic: aqueous) simulation box. red-water, blue-TiAP and cyan-dodecane.

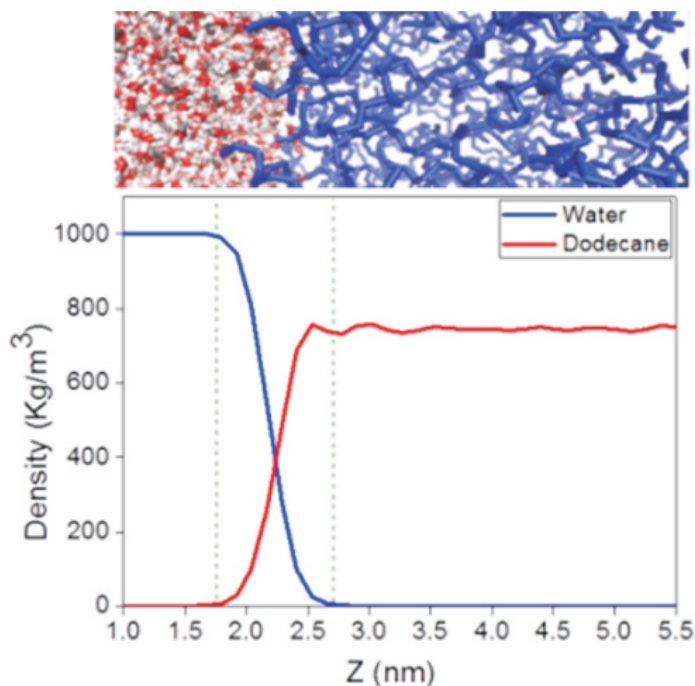


**Fig. 7:** Density profile of water–dodecane system (water: Red/White) and dodecane: Blue).

a good value of self-diffusivity of TiAP and a low value of shear viscosity.<sup>27</sup>

MD simulations in TiAP/dodecane mixture demonstrate that the Mulliken embedded force field captures most of the structural, dynamical and thermo-dynamical properties of ligand-solvent system. Therefore, it is also important to test this force field in biphasic mixture.<sup>27</sup> The starting simulation box is prepared by placing the ligand (TiAP) in the organic phase (dodecane) and water containing nitric acid as the aqueous phase as depicted in Fig. 6.

First, the force field is tested for simple water–dodecane system. The computed average bulk density of water and dodecane away from the interface is in quite good agreement with the reported experimental values.<sup>30</sup> A sharp interface is observed as displayed in Fig. 7.

In TiAP/dodecane–water biphasic system, the interface become sharper after 1500ps and TiAP molecules are accumulated at the interface which increases the interface roughness as well as interface area. The accumulation at the interface increases with increasing mole fraction leading to higher interfacial area (Fig. 8).<sup>30</sup>

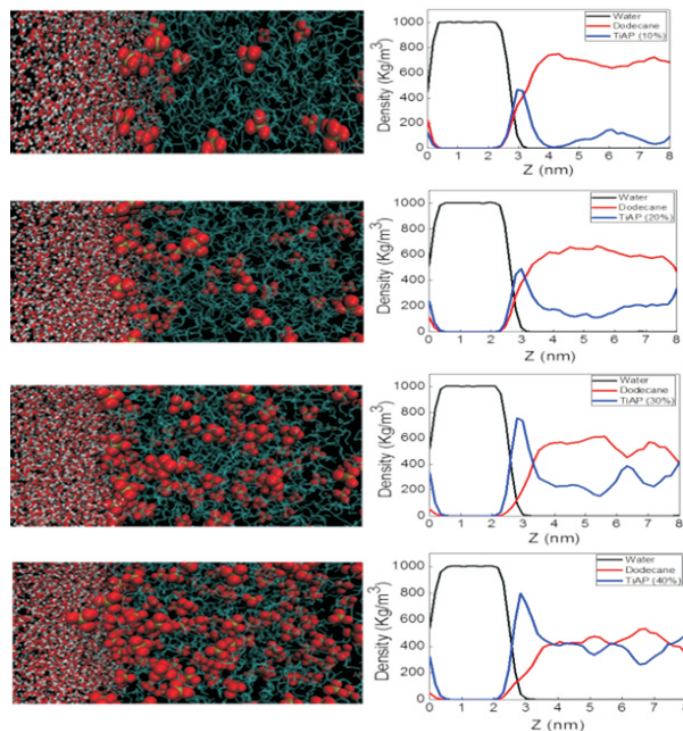


**Fig. 8:** Snapshot of liquid structure and density profiles for 10%, 20%, 30% and 40% of TiAP in dodecane–water system. Cyan: dodecane, Red & White: water, Red & Grey: phosphoryl group of TiAP.

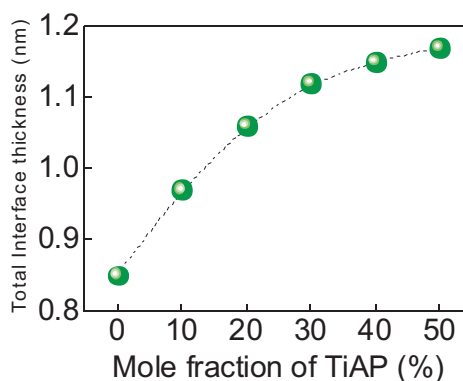


**Fig. 9:** Interface thickness vs. mole fraction of TiAP.

The interfacial thickness is seen to increase with TiAP in Fig. 9. The interface thickness is affected up to a certain mole fraction of TiAP (here 50%). Above 50%, it remains almost invariant and therefore further increase of TiAP will not help in the mass transfer.<sup>30</sup>

The interaction,  $E_{int}$  between water molecules is reduced in the presence of TiAP. The breakage of H-bond among water molecules reduces the surface tension of water which helps to increase the mingling of water and organic phases. Therefore, higher packing of TiAP at the interface accelerates the hydration of TiAP and thus leads to more reduction of the interfacial tension. The O–H bond (1.81Å) in TiAP–H<sub>2</sub>O complex (O of P=O and H of water molecule) is found to be quite smaller than O–H bond (2.16Å) in water dimer indicating that the TiAP–H<sub>2</sub>O interaction is stronger than that of H<sub>2</sub>O–H<sub>2</sub>O interaction as reflected in the interaction energy. The  $E_{int}$  for TiAP–H<sub>2</sub>O interaction (-10.74kcal/mole) is found to be higher than that of H<sub>2</sub>O–H<sub>2</sub>O interaction (-4.63kcal/mole) at the B3LYP/TZVP level of theory. The O–H bond length in TiAP–H<sub>2</sub>O complex (O of P=O and H of water) from MD simulation was found to be 1.55Å

**Table 1.** Interfacial tension (IFT) and interface thicknesses (IFW) of neutral biphasic system at T=300<sup>o</sup>K.

TiAP (%)	IFT (mN/m)		IFW (nm)		
	Simulation	Expt <sup>31</sup>	w <sub>c</sub>	w <sub>t</sub>	w <sub>i</sub>
0	49.3±1.6	52.6	0.202	0.767	0.740
10	28.7±2.0	35.3	0.261	0.996	0.961
20	27.1±2.3	25.5	0.268	1.03	0.994
30	24.4±2.9	20.5	0.283	1.091	1.054
40	23.2±2.1	18	0.291	1.126	1.088

whereas it is 1.95Å for water, which might be reasonable due to different physical state of the molecular system in MD and QM.<sup>30</sup>

The interface thickness is changed with acid and it exhibits a decreasing trend. The inverse relation between interfacial tension and interface thickness is established for water–TiAP/dodecane system [inset of Fig. 10]. They are related by capillary wave theory (CWT)<sup>32</sup> as

$$w_c^2 = \frac{k_B T}{2\pi\gamma} \ln\left(\frac{L_{II}}{L_b}\right) \quad (1)$$

here, w<sub>c</sub> is the interface thickness due to capillary wave, k<sub>B</sub> is Boltzmann constant, L<sub>II</sub> is the box dimension along x or y direction and L<sub>b</sub> represents bulk correlation length in terms of molecular length. The molecular diameter is evaluated from the volume determined by COSMOtherm program. The calculated w<sub>c</sub> (water–dodecane) was (0.20nm) very close to reported value of 0.33nm. In the presence of TiAP it is more appropriate to introduce the weighted average of TiAP and dodecane for L<sub>b</sub>.<sup>30</sup>

$$L_b = L_{W-T} * x_{TiAP} + L_{W-D} * x_{Dodecane} \quad (2)$$

L<sub>W-T</sub> and L<sub>W-D</sub> are the average molecular lengths considering water–TiAP and water–dodecane interface respectively. X<sub>TiAP</sub> and X<sub>dodecane</sub> are the mole fraction of TiAP and dodecane. Further, the total interface are the mole fraction of TiAP and dodecane. Further, the total interface thickness (w<sub>i</sub>) can be well fitted to an equation as follows:

$$w_t^2 = C \frac{k_B T}{\gamma} \ln\left(\frac{L_{II}}{L_b}\right) \quad (3)$$

$$C = \frac{(\sigma_{Water} + \sigma_{TiAP} + \sigma_{dodecane})}{1.4 \sigma_{water}} \quad (4)$$

w<sub>i</sub> obtained from the density curve and from the proposed equation (Eqn.3 & Eqn. 4) using the molecular length (L<sub>b</sub>) calculated from the weighted average method are in good agreement as shown in Fig.10 as a function of mole fraction of TiAP and acid concentration.<sup>30</sup>

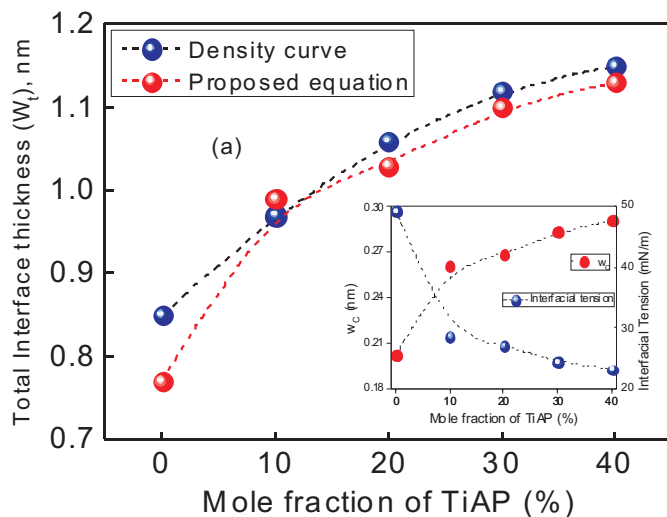


**Fig.10:** Total interface thickness as a function of mole fraction. Capillary thickness and interfacial tension vs. mole fraction of TiAP [inset of Fig 10].

The interface thickness calculated from the density profile is substantially high compared to w<sub>c</sub> indicating that w<sub>c</sub> is not the sole contributor. Hence, it is inappropriate to propose w<sub>c</sub> as the true interface thickness. The contribution from intrinsic thickness (w<sub>i</sub>) is obtained as:

$$w_i^2 = w_t^2 - w_c^2 \quad (5)$$

The calculated value of w<sub>i</sub> for water-dodecane system using Eqns. 3, 4 and 5, was 0.74nm which is very close to the reported MD simulation value of 0.51nm and thus confirms the approval of the model equation (Eqn.3 & Eqn.4).<sup>30</sup> The calculated w<sub>t</sub>, w<sub>c</sub> and w<sub>i</sub> for various compositions of TiAP and acidity are listed in Table 1. The predictability of the proposed equation for calculation of interface thicknesses (nm) lies within 60–70%.

The preferential orientation of phosphoryl group at the interface has also been evaluated. The interface has quite negligible effect on the orientation of water molecule while the orientation of TiAP molecule has been changed markedly in the presence of interface compared to pure state. From the snapshot it was seen that the phosphoryl oxygen from one TiAP unit is facing the back of the P of P=O of the neighboring TiAP unit (Fig.11).

Further, the stability of the dimer with different orientation was established by computing the dimerization energy by dispersion corrected DFT. The interaction energy for dimer with orientation of O=P-P=O, P=O-P=O and P=O-O=P was found to be -12.98, -14.97 and -10.81 kcal/mole respectively indicating that dimer with orientation of P=O-P=O is the most stable which was also captured

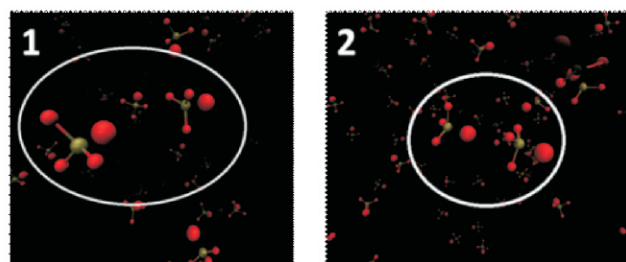


**Fig.11:** Preferential orientation (P=O-P=O) of phosphoryl group of TiAP molecules.

**Table 2.** Partial charges on U ( $q_U$ ) and O ( $q_O$ ) of uranyl.

Model	$q_U$ (e)	$q_O$ (e)
Model - MA(Mulliken)	2.719	-0.3595
Model - GW(Gulibaud and Wipff)	2.500	-0.2500
Model - ML(Mulliken -Liquid)	2.198	-0.0992
Model - MG(Mulliken -Gas)	2.033	-0.0164

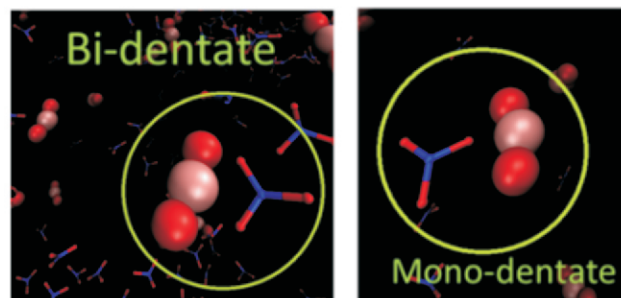


**Fig.14:** Snap shot of bi- and mono-dentate nitrate ions. Red-O, Blue-N and Pink-U.

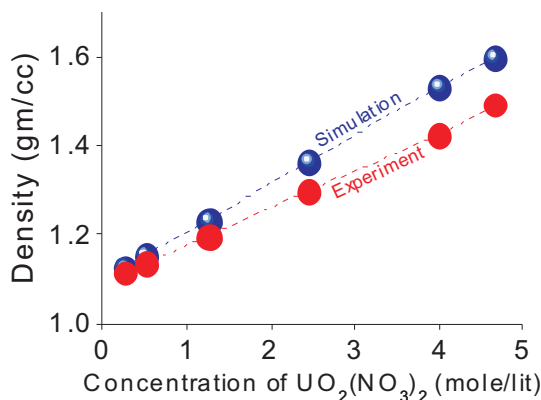


**Fig.12:** Density of uranyl nitrate solution in 3M nitric acid at various concentrations.

in the MD simulation.<sup>30</sup> The simulation studies in biphasic system also reveal that a single force field without parameterization is able to predict structural, dynamical and thermo-dynamical properties in pure, binary and biphasic system. Next, simulations were conducted to find out the limiting feed concentrations in PUREX process. The effects of partial charges on uranyl ion were studied to find out the correct model amongst available force fields (Table 2).

After calculation of structural, dynamical and thermo-dynamical properties for uranyl ion in water system it is observed that the variation in atomic charges does not have much significant effect on the force field except the free energy of hydration where the partial charges have significant effect. Here, GW model was chosen for the uranyl ions due to accurate hydration free energy. The systems considered here are for a wide range of uranyl nitrate concentration from 0.25-5.45 mole/lit in 3M nitric acid.<sup>33</sup> The calculated bulk densities of each system were found to increase with uranyl nitrate concentration. The experimental results exhibit an excellent agreement with the densities obtained from MD simulations (Fig. 12).

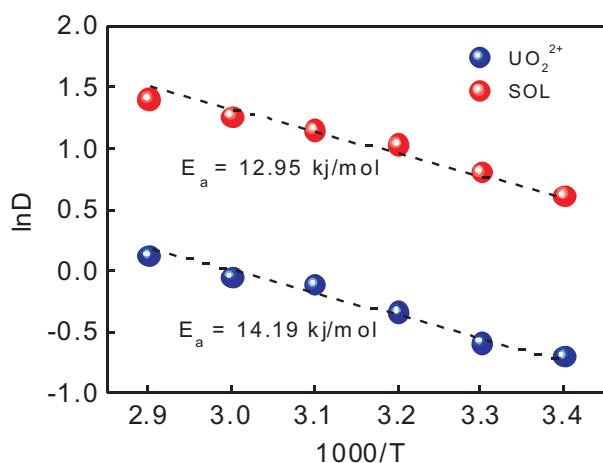


**Fig.13:** Arrhenius plot of diffusivity against temperature (uranyl nitrate:0.5 moles/lit).

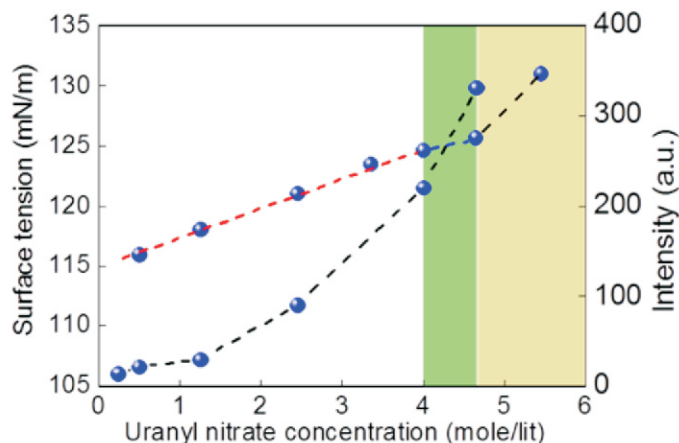


**Fig.15:** Calculated surface tension of uranyl nitrate solution and experimental intensity using DLS.

The diffusivity of  $UO_2^{2+}$  ion and water is decreased with uranyl nitrate concentration due to increased friction. The temperature dependency on self-diffusivity has also been studied using the Arrhenius equation<sup>34</sup> and the dependency is found to be linear as shown in Fig. 13.

The bi-dentate structure is formed at low concentration and mono-dentate at higher uranyl ion concentration. This is because more number of uranyl ions reduce the availability of nitrate ions around  $UO_2^{2+}$  and also there a competition between water and nitrate ion to occupy the first solvation shell<sup>33</sup>(Fig. 14).

Surface tension plays an important role in the liquid-liquid extraction and in particular in stripping operation of various interfacial processes. The computed surface tension is increased linearly with concentration of uranyl nitrate up to certain concentration as displayed in Fig.15. The nonlinearity starts appearing at higher concentration of 5.45 mole/liter where a deviation in surface tension is noted from monotonic linear increase. This phenomenon perhaps indicating the super saturation of uranyl nitrate at very high concentration which may drives the formation of crystal. In order to support the simulation findings, dynamic light scattering (DLS) experiment was conducted to explore the behavior of aqueous mixture. The scattering results (Fig. 15) display that homogeneity of solution is maintained up to 4.0 moles/lit and then becomes heterogeneous as the light fails to pass through the solution. The nonlinearity in the intensity curve is appeared at the same location where the nonlinearity in surface tension was observed. Similar deflection in shear viscosity was also observed from 4.5–5.45 mole/lit indicating a possible super saturation phenomena.

## Conclusion

The MD simulation studies have been performed in wide range of aqueous and organic mixtures along with pure component to establish the TiAP as a potential ligand and at the same time to develop a single force field which can capture all the properties. The Mulliken charge embedded force field was able to explain all the properties in bulk liquid phase as well as in interface. The present article concludes that TiAP might be considered as an alternate of TBP.

## Acknowledgements

Computer Divison, BARC is acknowledged for Anupam super computation facility. The authors are grateful to K.T. Shenoy, Group Director, Chemical Engineering Group and S. Mukhopadhyay, Head, Chemical Engineering Division for encouragement. Sincere thanks to all experimental collaborators.

## Corresponding Author\*

Sk. Musharaf Ali (musharaf@barc.gov.in)

## References

- [1] M. Simpson, and J. Law, *Nuclear Fuel Reprocessing. Idaho National Laboratory*, INL/EXT-10-17753, 2010.
- [2] S.H. Hassan, J.P. Sukla, *J. Radioanal. Nucl. Chem.*, 2003, **258**, 563–573.
- [3] S. Cui, V.F. de Almeida, B. Khomami, *J. Phys. Chem. B*, 2014, **118**, 10750- 10760.
- [4] J. Mu, R. Motokawa, C.D. Williams, K. Akutsu, S. Nishitsuji, and A. Masters, *J. Phy. Chem. B*, 2016, **120**, 5183–5193.
- [5] S. Cui, V.F. de Almeida, B.P. Hay, X. Ye, B. Khomami, *J. Phys. Chem. B*, 20, 12, **116**, 305- 313.
- [6] S.W.L. Siu, K. Pluhackova, R.A. Bockmann, *J. Chem. Theory Comput.*, 2012, **8**, 1459- 1470.
- [7] Q.N. Vo, L.X. Dang, M. Nilsson, H.D. Nguyen, *J. Phys. Chem. B*, 2016, **120**, 6985- 6994.
- [8] L. Leay, K. Tucker, A.D. Regno, S.L.M. Schroeder, C.A. Sharrad, A. Masters, *J. Mol. Phys.*, 2014, **112**, 2203–2214.
- [9] W. Allen, and R.L. Rowley, *J. Chem. Phys.*, 1997, **106**, 10273–10281.
- [10] M. Baden, M. Burgard, G. Wipff, *J. Phys. Chem. B*, 2001, **105**, 11131–11141.
- [11] P. Sahu, Sk. M. Ali, K.T. Shenoy, *Chemical product and process modelling* 2017.
- [12] B. Wen, C. Sun, B. Bai, E.Y. Gatapova, O.A. Kabov, *Phys. Chem. Chem. Phys.*, 2017, **19**, 14606–14614.
- [13] R. Biswas, P. Ghosh, T. Banerjee, Sk. M. Ali, K.T. Shenoy, *J. Mol. Liq.* 2017, **241**, 279–291.
- [14] M. Jorge, and M.N.D.S. Cordeiro, *J. Phys. Chem. C*, 2007, **111**, 17612–17626.
- [15] S. Senapati, and M.L. Berkowitz, *Phys. Rev. Lett.*, 2001, **87**, 176101-1-4.
- [16] P. Guilhaud, and G. Wipff, *J. Mol. Struct.*, 1996, **366**, 55–63.
- [17] S. Kerisit, and C. Liu, *J. Phys. Chem. A*, 2013, **117**, 6421–6432.
- [18] N. Rai, S.P. Tiwari, and E.J. Maginn, *J. Phys. Chem. B*, 2012, **116**, 10885–10897.
- [19] M.P. Allen, D.J. Tildesley, *Computer Simulation of Liquids*, 2017: Clarendon Press, Oxford University.
- [20] A. D. Becke, *Phys. Rev. A*, 1988, **38**, 3098-3100.
- [21] TURBOMOLE V6.6. a development of University of Karlsruhe and Forschungszentrum Karlsruhe GmbH, 1989- 2007, TURBOMOLE GmbH, since 2007.
- [22] M.F. Guest, I.J. Bush, H.J.J. Van Dam, P. Sherwood, J.M.H. Thomas, J.H. Van Lenthe, *Mol. Phys.*, 2007, **103**, 719-747.
- [23] J. Mark, M.J. Abraham, J.E. Gready, *J. Comput. Chem.*, 2011, **32**, 2031–2040.
- [24] A.P. Sunda, and A. Venkatnathan, *Mol. Simu.*, 2013, 1–6.
- [25] T. Straatsma, H., Berendsen, *J. Chem. Phys.*, 1988, **89**, 5876–5886.
- [26] A. Das, P. Sahu, Sk. M. Ali, *J. Chem. Eng. Data*, 2017, **62**, 2280–2295.
- [27] A. Das, and Sk. M. Ali, *J. Chem Phys.*, 2018, **148**, 074502-1-14.
- [28] G. Peskir, *Stoch. Models*, 2003, **19**, 383–405.
- [29] B. Hess, *J. Chem. Phys.*, 2002, **116**, 209–217.
- [30] Das, A. and Ali, Sk. M., *J. Mol. Liq.*, 2019, **277**, 217–232.
- [31] M.L. Singh, S.C. Tripathi, M. Lokhande, P.M. Gandhi, and V. G. Gaikar, *J. Chem. Eng. Data*, 2014, **59**, 1130–1139.
- [32] F. Buff, R. Lovett, F. Stillinger, *Phys. Rev. Lett.*, 1965, **15**, 621–623.
- [33] A. Das, Sk. M. Ali, *J. Phys. Chem. B*, 2019, **123**, 4571- 4586.
- [34] C. D'Agostino, R.C. Harris, A.P. Abbott, L.F. Gladden, M.D. Mantle, *Phys. Chem. Chem. Phys.*, 2011, **13**, 21383- 21391.
- [35] R. Walser, A.E. Mark, W.F. van Gunsteren, *Chem. Phys. Lett.*, 1999, **303**, 583–586.
- [36] P. Banerjee, S. Yashonath, B. Bagchi, *J. Chem. Phys.* 2017, **146**, 164502.
- [37] J.P. Hansen, I.R. McDonald, *Theory of Simple Liquids* (Academic Press, NewYork, 1986).